

Received 31 July 2023, accepted 10 September 2023, date of publication 13 September 2023,
date of current version 20 September 2023.

Digital Object Identifier 10.1109/ACCESS.2023.3315117

RESEARCH ARTICLE

A Novel C/X-Band Linear Polarized Conformal Shared Aperture Antenna Array for Spaceborne SAR Applications

BALA ANKAIHAH NUNNA¹, (Graduate Student Member, IEEE), AND
VENKATA KISHORE KOTHAPUDI¹, (Senior Member, IEEE)

Center of Excellence Advanced RF Microwave and Wireless Communications, Department of Electronics and Communication Engineering, School of Electrical, Electronics and Communication Engineering, Vignan's Foundation for Science, Technology, and Research (VFSTR), Vadlamudi, Guntur, Andhra Pradesh 522213, India

Corresponding author: Bala Ankaiah Nunna (balaankaiah@ieee.org)

ABSTRACT In this work, a dual-band linear polarized C/X conformal shared aperture antenna (SAA) for spaceborne SAR applications is presented. The proposed single layer SAA is designed with a square-shaped patch in linear polarization and arranged as four elements (2×2) array with corporate feeding to allow for efficient signal transmission. The design of that operates at C-band (5.35 GHz) and X-band (9.65 GHz). Most spaceborne applications, such as satellite radar and weather forecasting, employ the C-band antenna. On the other hand, X-band antennas are used for surveillance, reconnaissance, air traffic control, and weather monitoring. A prototype is built, and its s-parameters are tested to confirm the antenna. With the suggested design, we were able to obtain a bandwidth of 65 MHz for C-band and 354 MHz for X-band, as well as gains of 13.2 dBi for the C-band and 10.6 dBi for the X-band, and isolation of more than 40 dB. The total size of the SAA is $130 \times 80 \times 0.8$ mm. According to this study, dual band antennas operating on future SAR spacecraft on a same aperture is a practical solution to satisfy user demands.

INDEX TERMS Conformal antenna, shared aperture antenna, linear polarization, corporate feed, spaceborne, synthetic aperture radar.

I. INTRODUCTION

The requirements of the SAR systems have a major role in creating high demands on the antennas performance, which is to be considered while designing a system. SAR's have been used extensively in earth monitoring satellites. Historically, all satellites platforms have incorporated with the SAR in space within a monostatic system. As mentioned, same antenna was used for transmission and reception. In this paper, the research is focused on the design of SAR antenna with dual-band linear polarization for C-band and X-band with a single physical aperture. Most of the space-borne SAR systems use mechanical beam steering or phase-arrays to maximise azimuth coverage. And most of the tiny satellite SAR systems now operate on a single band,

The associate editor coordinating the review of this manuscript and approving it for publication was Hussein Attia¹.

which restricts the information. It has been stated that several dual-band dual-polarized antennas exist throughout the past two decades. Dual frequency operating with a single aperture will be necessary for the sophisticated SAR antennas in the future. Active phased array antennas with hundreds of dual polarised sub arrays will be used in upcoming spacecraft SARs. Additionally, it is preferred that the dual-polarization, dual-frequency antenna be able to operate simultaneously. A small, inexpensive spacecraft can only be equipped with a single aperture antenna. Conformal antennas with numerous elements are frequently used in SAR spaceborne applications because they may produce a variety of shaped beams, including nulls and side-lobe areas with complex shapes.

In this paper [1], a low-profile 8×8 conformal series-fed microstrip array is designed and analyzed for aircraft application. The achieved bandwidth is about 12% with

a VSWR less than 2.3. This paper presents the design of conformal Magneto-Electric dipole antenna for Sub 6 GHz application [2]. In the lower band, this design achieves 54.2% bandwidth and gain of 6.05 dBi, whereas in the upper band, it is 9.2%, with a gain of 5.71 dBi, are observed respectively. In this paper [3], for the global navigation satellite system, a dual-band non-planar antenna is given. When compared to bent traditional two feeds patch antennas, the results demonstrate comparatively good in terms of gain and axial-ratio. For airborne applications, a dual band dual polarization antenna is introduced in this paper [4]. Each 10 GHz and 3 GHz antennas are a circular patch and rectangular ring resonator antenna with a gain of 18.3 dBi and 9.5 dBi respectively. This paper presents the design of 4×4 conical conformal microstrip array [5]. This element is coupled with a parallel feed network to generate a conformal microstrip array on a cone surface. In this paper [6], broadband conformal phased array with optical beam forming for airborne satellite communication is presented. A parasitic element is layered on top of a lower patch of the Ku-band antenna, which is separated from it by designated space filler. A conformal antenna with low RCS is proposed in [7]. A dual-ring configuration of meta-cells is built around the central antenna. In this paper [8], conical missile-borne applications need for the use of a dual-band conformal antenna that can receive both GPS L1 and Beidou B3 signals.

This paper presents a conformal MIMO antenna with DGS structure that operates at dual frequencies for wireless application [9]. The proposed antennas have resonated at 9.49 GHz and 11.8 GHz and the return loss is less than -10 dB. The proposed antennas have good gain and radiation characteristics observed. Synthesis of conformal arrays for SAR applications is presented in [10]. The study presents the specifications and the design of a cutting-edge dual polarized of the space-borne SAR antenna utilizing aperture-coupled microstrip patch components [11]. The cross-polarization level is below -23.1 dB and the active reflection coefficient is below -15 dB throughout a bandwidth of 150 MHz and elevation scan volume of 15 degree. This paper [12] presents a dual-band conformal antenna that resonates in the 2.4 GHz and 5.8 GHz frequency bands for lower- and higher-frequency WLAN. In [13], a meander line monopole antenna for unmanned aerial vehicle is presented. When operating at 780-900 MHz and 1.2-2.28 GHz, the antennas achieve the omnidirectional radiation pattern. This paper depicts the radiating component of the conformal adaptive antenna of various planar arrays [14]. An integrated dual-band antenna is presented in this paper for usage in spacecraft [15]. The development of the L- and S-band antenna with axial ratio of less than 3 dB and return loss ranging from 15 dB to 22 dB are the characteristics of the intended developed antenna. In this paper [16], for applications involving space-borne digital beamforming (DBF) synthetic aperture radar (SAR), a X/Ka-band SAA is presented. The Ka-band sub array at

9.6 GHz and X-band antenna at 35.75 GHz are interlaced on the same plane to share an aperture. This paper [17] presents a variety of strategies for putting into practice a shared-aperture dual-frequency dual-polarized array antenna for space-based synthetic aperture radar (SAR) applications. Typically, side lobe values in azimuth were obtained at -12 dB. The cross polar level for the X-band array is roughly -18 dB and was less than -21 dB for the C-band antenna. It is reported on two types of innovative dual band antennas that are appropriate for data communication devices in [18]. A multidisciplinary Earth-observing radar program called NISAR performs around the globe measurements of land surface changes that will significantly enhance Earth system models [19]. The S-SAR equipment, spacecraft bus, and launch vehicle are all provided by ISRO [20].

In this paper [21], a dual-CP spherical conformal phased array antenna (SPAA) for the S band is created. In the course of research, an innovative idea of dual- and tri-band conformal capsule antennas are inducted as suggested in [22]. The usefulness and need of spaceborne SAR Systems has become obvious [23]. In [24], describes the development of the core SAR-XL technology and presents the test results for demonstrating the functionality and performance. The GPS L1, L2, and GLONASS L1 signals are presented in this study together with a two-element conformal antenna for use in precision artillery applications [25]. This research introduces a unique X/Ka-band dual-polarized DBF-SAR system [26]. The microstrip antenna arrays with the double-sided are presented in [27]. This design achieves the performance of 3.12 dBi gain at 6.5 GHz and 3.8 dBi gain at 9.5 GHz. An innovative dual band dual polarized shared-aperture antenna is presented in this study with possible uses in synthetic aperture radars (SARs) [28]. A gain of 21.4 dBi in horizontal polarization and 21.2 dBi in vertical polarization was measured. In this paper [29], a novel DBDP antenna with low frequency ratio is proposed. The polarization is measured to have directivities of 24.7 dBi and 29.2 dBi. The development of a single-feed, circularly polarized antenna with broad axial ratio (AR) bandwidth is given in [30]. The side lobe levels are -12.5 dB and -15 dB for C-band and X-band respectively; high gain values are for C-band is 14.5 dBic and 17.5 dBic for X-band. In this paper [31], Simulated C-band and X-band working antenna elements include 4-element sub-arrays. Both the 6 GHz and 10 GHz antennas have gains of 11.3 dB and 12.4 dB, respectively.

On a FR-4 substrate, a 1×8 dual band antenna array operating at 5.8 GHz and 9.65 GHz has been designed for SAR on UAV applications is presented in [32], respectively. At C-band, the gain is 6.39 dBi, while at X-band, it is 3.825 dBi. In [33] and [34], presents the design of X band antenna array with different element configurations. In [35], designed the single layer conformal SAA for C/X-bands. Machine learning and deep learning for various antenna

designs is explained in [36] and [37]. In [38] and [39] dual band antennas and conformal phased array antennas for are explained.

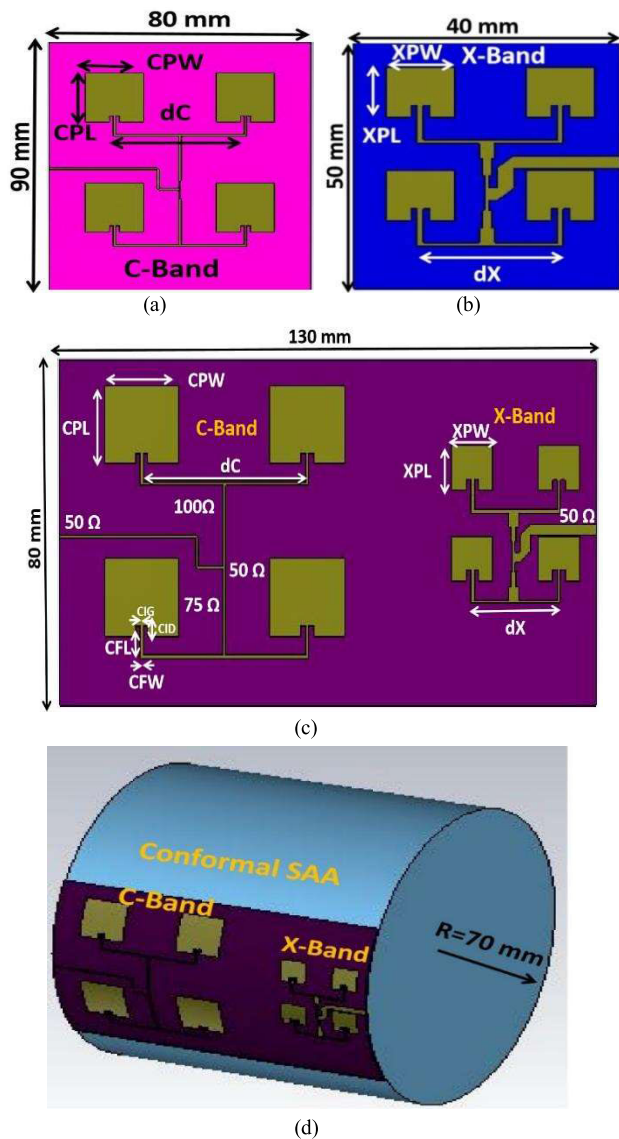


FIGURE 1. (Geometrical configuration of dual band conformal SAA: (a) C-band (b) X-band (c) SAA with C/ X-band (d) Conformal SAA with C/ X-band.

Considering the literature analysis as mentioned earlier, we shall suggest an extended version of the above single layer conformal dual band, linear polarized, 2×2 corporate fed SAA for C/X-bands. The suggested antenna is built for 5.35 GHz for the C-band and 9.65 GHz for the X-band frequencies. Full-wave simulations of the proposed antenna are run using the industry-recognized FFT-based CST MWS software 2021 to analyze it. The suggested antenna has been built and tested. Section II talks about the suggested antenna structure and design, while Section III talks about the results of simulations and experiments. Section IV discusses the conclusions in detail.

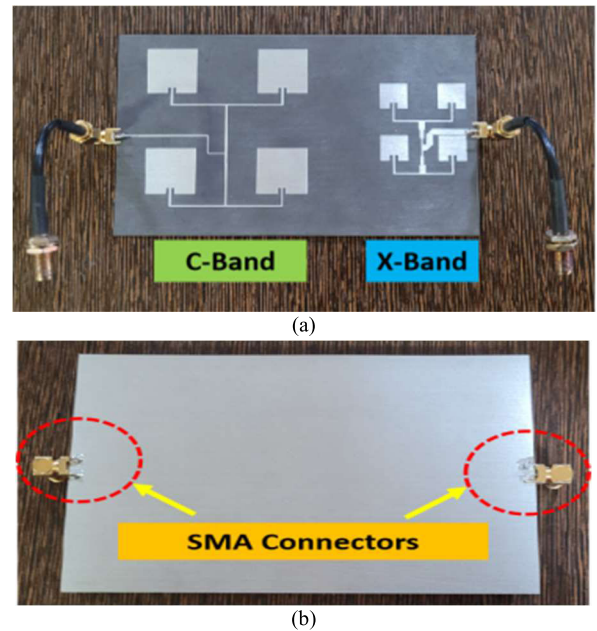


FIGURE 2. C/X-Band planar shared aperture antenna array (a) Top view (b) Bottom view.

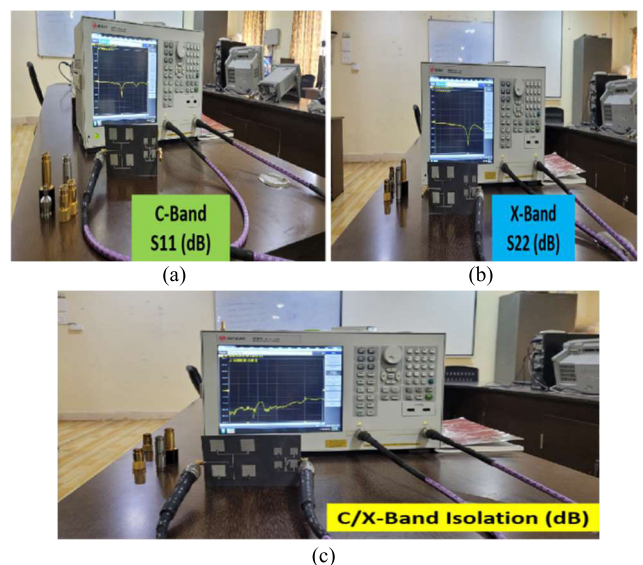


FIGURE 3. Measurement of VNA for C/X-Band Planar SAA (a) C-Band measurement of S11 (b) X-Band measurement of S22 at (c) measurement of isolation S12.

II. STRUCTURE OF THE PROPOSED SHARED APERTURE ANTENNA ARRAY DESIGN

The proposed antenna's configuration consists of two dual-band antennas, one operating at 5.35 GHz for C-band frequency and the other at 9.65 GHz for X-band frequency. In this study, a dual band C/X conformal SAA for spaceborne SAR is proposed. It has linearly polarized in the C-band at 5.35 GHz and X-band at 9.65 GHz with 2×2 elements respectively. In both C-band and X-band antennas, we have used square-shaped patches to lower the antenna's losses

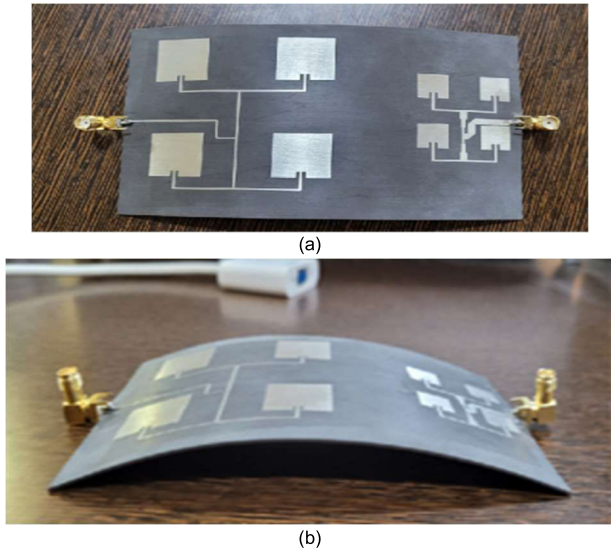


FIGURE 4. C/X-Band conformal shared aperture antenna array (a) top view (b) side view.

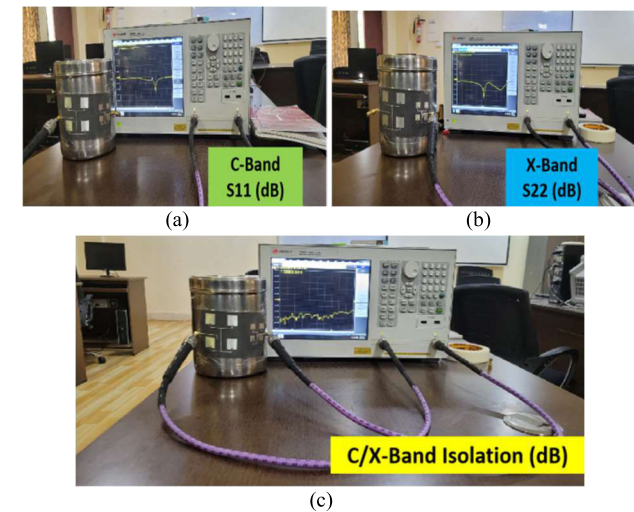
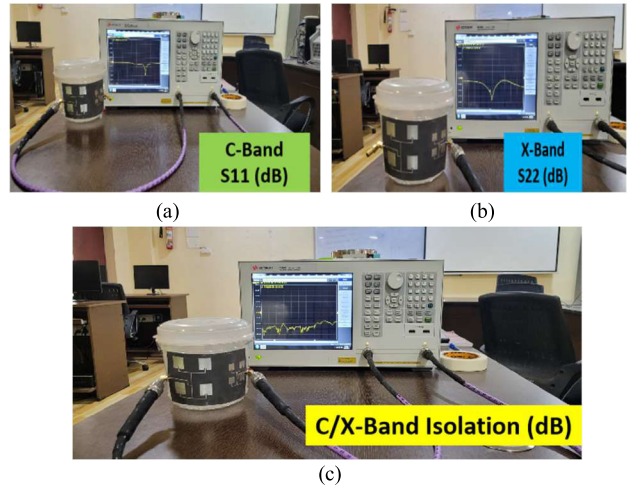


FIGURE 5. Measurement of VNA for C/X-Band conformal SAA with 70 mm (a) C-Band measurement of S11 (b) X-Band measurement of S22 (c) measurement of isolation S12.

while transmitting. CST MWS software was used to do the simulations. In arrays, the antenna inter element spacing is assumed to be 0.7λ . This study considers the $\tan\delta = 0.0009$ with the RT/Duroid-5880 substrate, and all designs use a $\epsilon_r = 2.2$.

Fig. 1 (a) depicts the linear polarisation configuration of the C-band array antenna with all its parameters. In Fig. 1(b), the X-band array antenna's configuration is depicted.

Both the array antennas ports are excited using microstrip line feeding. Then both bands are combined into a single aperture. Following is a representation of the geometrical configuration of the C/X-band SAA with the evolving stage in Fig. 1 (c). To compare well with other systems, this shared

FIGURE 6. Measurement of VNA for C/X-Band conformal SAA array with 60 mm (a) C-Band measurement of S11 (b) X-Band measurement of S22 (c) measurement of isolation S12 (d) measurement setup of radiation pattern for C/X-Band conformal SAA array.

aperture antenna array is curved on cylinders of various radii. The conformal SAA's design is displayed in Fig. 1 (d). Table 1 displays the final, optimised values of the proposed C/X-band SAA.

A. PLANAR SHARED APERTURE ANTENNA ARRAY

Fabricated C/X-band Planar Shared aperture antenna array top view and bottom views are shown in Fig. 2(a) and Fig. 2(b). Measurement of VNA for C/X-band Planar SAA array is shown in Fig. 3. C-band S11 measurement and X-band S22 measurement is shown in Fig. 3(a), 3(b) and isolation measurement is presented in Fig. 3(c).

TABLE 1. Optimized parameters.

C-Band (5.35 GHz)		X-Band (9.65GHz)	
Parameter	Value(mm)	Parameter	Value mm)
CPL	18	XPL	10
CPW	18	XPW	10
CFL	5.5	XFL	5.5
CFW	1.0	XFW	1.0
CIG	1.0	XIG	1.0
CID	2.4	XID	2.4
dC	40	dX	22

CPL = Patch Length of C-Band
 CPW = Patch Width of C-Band
 CFL = Feed Length of C-Band
 CFW = Feed Width of C-Band
 CIG = Inset Gap of C-Band
 CID = Inset Distance of C-Band
 dC = Inter element spacing of C-Band

XPL = Patch Length of X-Band
 XPW = Patch Width of X-Band
 XFL = Feed Length of X-Band
 XFW = Feed Width of X-Band
 XIG = Inset Gap of X-Band
 XID = Inset Distance of X-Band
 dX = Inter element spacing of X-Band

B. CONFORMAL SHARED APERTURE ANTENNA ARRAY

The top view and side view of the constructed C/X-band conformal SAA array are illustrated in Figures 4(a) and 4(b), respectively. To outperform the competing systems, this SAA array was bent on a cylinder with a different radius. The conformal SAA bent on a 60 mm and 70 mm radius cylinder as depicted below.

Measurement of VNA for C/X-band conformal shared aperture antenna array with a radius of 70 mm is shown in Fig. 5. S11 measurement at C-band and S22 measurement at X-band is shown in Fig. 5(a), 5(b) and isolation measurement is shown in Fig. 5(c).

Measurement of VNA for C/X-band conformal SAA array with a radius of 60 mm is shown in Fig. 6. C-band S11 measurement and X-band S22 measurement is shown in Fig. 6(a), Fig. 6(b) and isolation measurement is shown in Fig. 6(c). Measurement setup of radiation pattern for C/X-band conformal SAA is displayed in Fig. 6(d).

The spacing is calculated from equation (1)

$$d = \frac{\lambda}{1 + \sin\theta} \tag{1}$$

Here λ = wavelength in free space
 d = element spacing
 $\theta = 25^\circ$ scan angle.

III. SIMULATED AND EXPERIMENTAL RESULTS AND ANALYSIS

To validate the design, a prototype dual C/X band dual polarisation array with 5.35 GHz for the C- band and 9.65 GHz for the X-bands is designed and validated. This design is constructed and validated. C/X bands are lavished

on the prototype. CST Microwave Studio is the application software used to run each simulation. The S-parameters are measured using a key sight microwave vector network analyser. Fig. 7(a) and 7(b), respectively, depict the C/X-band SAA surface current distribution of the planar array for both C and X-bands. C/X-band SAA array surface current distribution of the conformal is shown in Figs. 8(a) and 8(b) respectively, for C and X-bands.

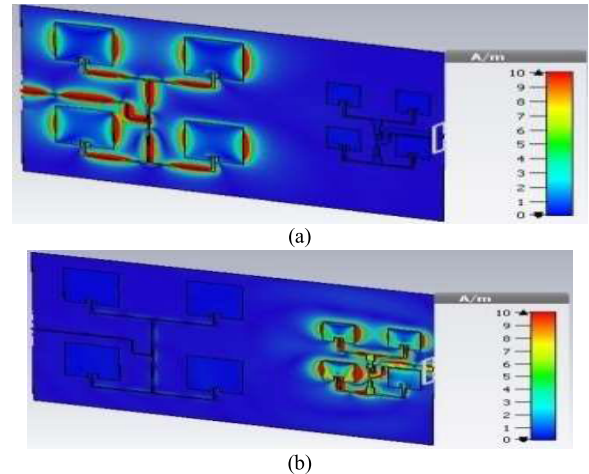


FIGURE 7. Planar SAA Surface current distribution of C/X-band for both ports (a) C-band (b) X-band.

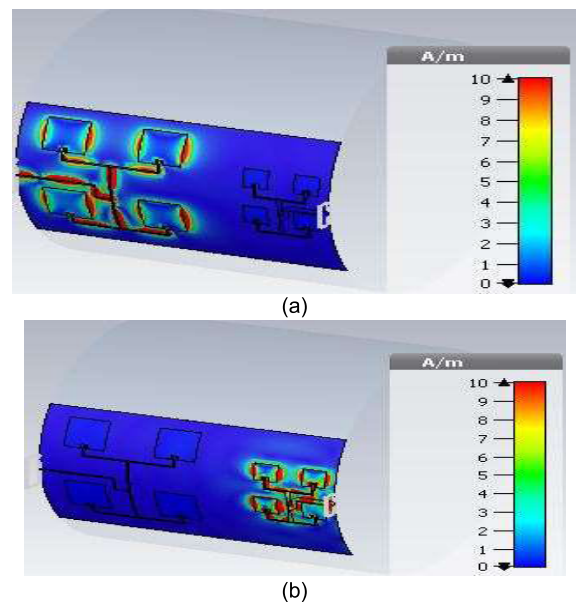


FIGURE 8. Conformal SAA surface current distribution of C/X-band for both ports (a) C-band (b) X-band.

The proposed C/X-band SAA array’s computed and observed return loss at C and X-bands are illustrated in Figs. 9(a) and 9(b) for both planar and conformal SAA. According to the results, the bandwidth for C-band is 60 MHz and return loss -27.05 dB for the planar array. After the entire SAA array conforming on a cylinder with a radius of 70 mm

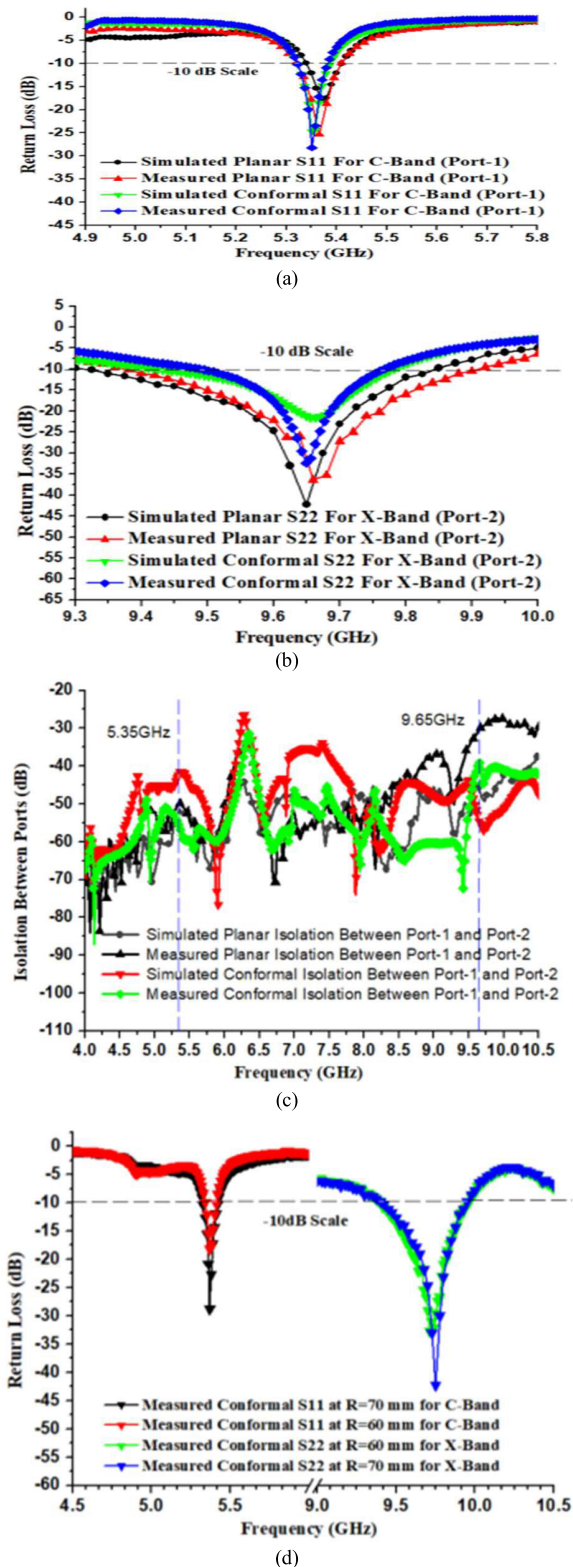


FIGURE 9. C/X-band SAA simulated and measured S-parameters of (a) S11 at C-band (b) S22 at X-band (c) Isolation S12 (d) S-parameters at R = 70 mm and R = 60 mm.

bandwidth is 65 MHz and the return loss is -24.67 dB. Like the return loss and impedance bandwidth for the X-band in planar are -32.38 dB and 280 MHz, respectively, the

return loss and impedance bandwidth after conforming on the cylinder are -21.45 dB and 354 MHz for both the X-band and the C-band, the return loss has been compared with planar. The results are consistent with both simulated and realised antenna configurations. The simulated and measured isolation for the C/X-band SAA with planar and conformal is shown in Fig. 9(c). Isolation is achieved more than -40 dB in both C/ X-bands. Fig. 9(d) shows the return loss with different radius of 70 mm and 60 mm.

The horizontally polarized Port 1 is utilized for the 2×2 corporate feed antenna arrays, and it resonates at a frequency of 5.35 GHz (C-band). The port's isolation is 56 dB, while port 1's return loss is -27.05 dB at 5.35 GHz. The simulated antenna radiation patterns measure at both the C- and X-bands. The C-band antenna radiation patterns at port-1 5.35 GHz, which consists of two planes. $\Phi = 0^\circ$ is E-plane and $\Phi = 90^\circ$ is H-Plane are shown in Fig. 10(a) and (b).

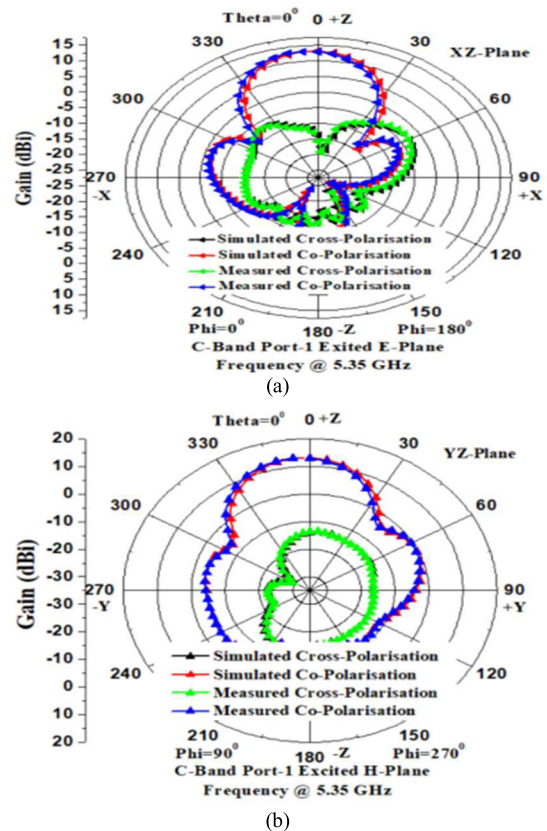


FIGURE 10. Conformal C/X-band SAA Simulated and measured radiation pattern of (a) E-Plane C-band (b) H-Plane C-band.

For the 2×2 corporate feed antennas, Port 2 is horizontally polarized and resonates at 9.65 GHz frequency (X-band). The port's isolation is -54.8 dB, while port 2's return loss is 32.38 dB at 9.65 GHz. In the same way antenna radiation patterns measured for X-band as well.

The simulated radiation patterns of the X-band antenna at port-2 of 9.65 GHz frequency with E-plane $\Phi = 0^\circ$ and

TABLE 2. Summary of results.

Parameters	C-Band				X-Band			
	Planar		Conformal		Planar		Conformal	
Frequency	5.35 GHz				9.65 GHz			
Polarization	Linear				Linear			
Return Loss (dB)	Simulated	Measured	Simulated	Measured	Simulated	Measured	Simulated	Measured
Isolation (dB)	-27.05	-17.8	-24.67	-15.4	-32.38	-26.0	-21.45	-19.0
Gain (dBi)	-56.0	-50.0	-42.0	-51.4	-39.38	-30.8	-54.8	-45.7
SLL (dB)	14	13	13.2	12.1	11.7	10.8	10.6	9.7
Antenna size	-14.3	-13.4	-13.6	-12.5	-12.3	-11.4	-15.9	-14.8
	130×80×0.8 mm ³							

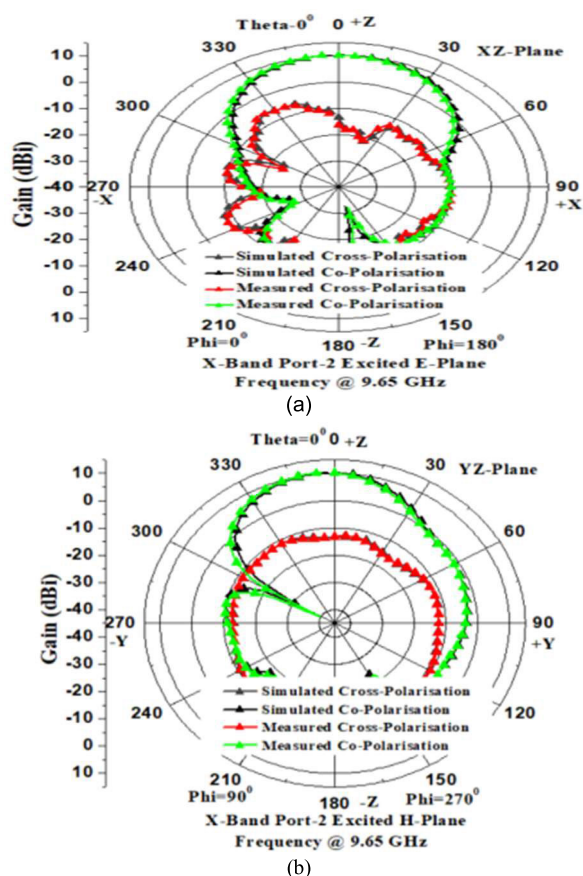


FIGURE 11. Conformal C/X-band SAA simulated and measured radiation pattern of at X-band (a) E-Plane X-band (b) H-Plane X-band.

H-Plane $\Phi = 90^\circ$ are shown in Fig. 11 (a) and (b). With the directional features, there is good agreement between the findings of the simulation and the measurements. At these two frequencies, it can be observed that the broadside radiation peak occurs. The polarization levels at 5.35 GHz in the E-Plane and H-planes are below -15 dB and at 9.65 GHz

frequency the polarization levels are below -15 dB. The simulated side lobe level for C-band is at -13.6 dB in E-Plane and H-planes at 9.65 GHz the SLL is -15.9 dB in the $\Phi = 0^\circ$ and $\Phi = 90^\circ$. Gain can be increased by increasing the antenna elements.

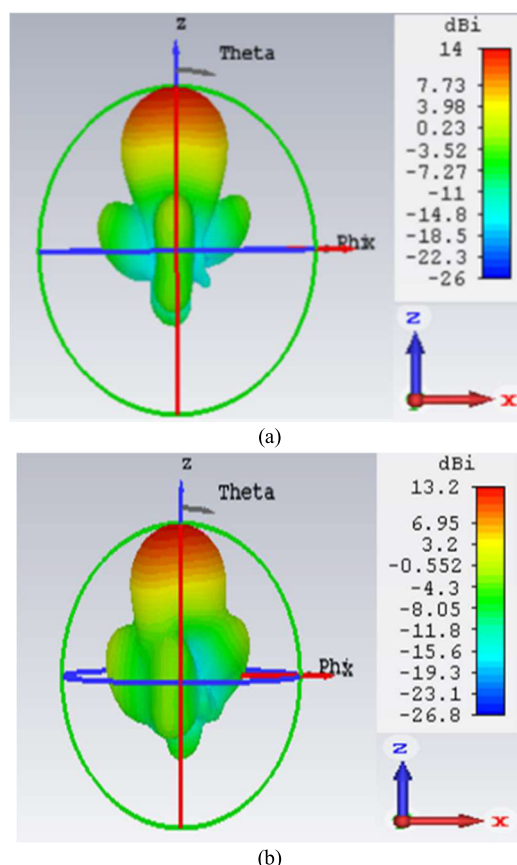


FIGURE 12. Simulated far field gain of C/X-band SAA at C-band (a) planar (b) conformal.

The C-band 3D far-field gain for planar SAA is shown in Fig. 12(a) and for conformal SAA is shown in 12(b). The

TABLE 3. Performance comparison.

Sl. No.	Year	Operation Bands	Frequency Ratio	Antenna Type	Configuration	Gain (dBi)	SLL (dB) Band 1/ Band 2	Aperture Size (mm)
[1]	1998	C / X (5.3 / 9.6)	1.8	Planar	Single Layer	NA	-12	NA
[2]	2013	C / X (6.5 / 9.5)	1.4	Planar	Single Layer	3.12 / 3.8	NA	NA
[3]	2016	C / X (5.3 / 9.6)	1.8	Planar	Multi Layer	16.2 / 21.2	-14.5 / -14.8	140 x 140 x 48mm ³
[4]	2017	C / X (5.2 / 10)	1.9	Planar	Single Layer	24.7 / 28.6	-15 / -20	NA
[5]	2017	C / X (5.3 / 8.2)	1.54	Planar	Multi Layer	14.5 / 17.5	-12.5 / -15	110 x 110 x 4.6mm ³
[6]	2019	C / X (6 / 10)	1.66	Planar	Single Layer	11.3 / 12.4	NA	NA
[7]	2019	C / X (5.8 / 9.65)	1.66	Planar	Single Layer	9.11 / 5.37	NA	220 x 50 x 1.6 mm ³
This Work		C / X (5.35 / 9.65)	1.80	Conformal	Single Layer	13.2 / 10.6	-13.6 / -15.9	130x80x0.8 mm ³

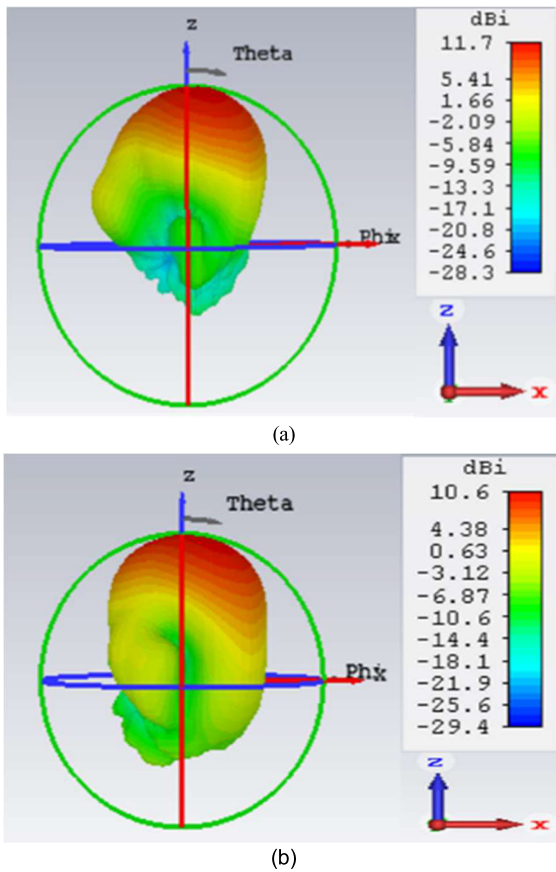


FIGURE 13. Simulated far field gain of C/X-band SAA at X-band (a) planar (b) conformal.

simulated gain is 14 dBi and the SLL is -14.3 dB for planar array, and the gain is 13.2 dBi and the SLL is 13.6 dB for a conformal array. The X-band 3D far-field gain for planar SAA is shown in Fig. 13 (a) and for conformal SAA illustrate at 13(b) respectively. Planar array simulated gain is 11.7 dBi and Side lobe level is -12.3 dB, while conformal SAA array simulated gain is -10.6 dBi and side lobe level is -15.9 dB. Table 2 summary are the obtained results. Comparing the proposed conformal SAA to other SAAs is shown in Table 3.

A novel SAA design with suitable performance attributes is confirmed by the prototype.

IV. CONCLUSION

This paper includes the proposed C/X-band conformal SAA corporate feed antenna for spaceborne SAR applications. Due to its adaptability, the cylinder is the shape that conformal antennas are employed most frequently. As, conformal antennas have the capability to bend on different platforms in spacecraft. To operate in satellites and UAV drone radars with large apertures, conformal antennas and arrays like AESA or multi-mode radars are required. Numerous benefits come with the suggested conformal SAA. In the C-band, it obtains a 13.2 dBi gain and side lobe level is -13.6 dB, and at X-band 10.6 dBi gain and side lobe level of -15.9 dB. This demonstrates the reliable performance of the conformal antenna arrays. The suggested conformal SAA array is appropriate for a range of stealth aircrafts, including placement on both spacecraft and aircrafts.

ACKNOWLEDGMENT

The authors would like to thank all the support that the department and university administration gave them to complete this task.

REFERENCES

- [1] Y. F. Qiang, L. Guo, Q. C. Zhu, and Y. F. Yao, *A Conformal Low-Profile Series-Fed Microstrip Array for Aircraft Applications*. Suzhou, China: IEEE, 2017.
- [2] B. Feng, K. L. Chung, J. Lai, and Q. Zeng, "A conformal magneto-electric dipole antenna with wide H-plane and band-notch radiation characteristics for sub-6-GHz 5G base-station," *IEEE Access*, vol. 7, pp. 17469-17479, 2019, doi: 10.1109/ACCESS.2019.2896356.
- [3] K. A. Yinusa, "A dual-band conformal antenna for GNSS applications in small cylindrical structures," *IEEE Antennas Wireless Propag. Lett.*, vol. 17, no. 6, pp.1056-1059, Jun. 2018, doi: 10.1109/LAWP.2018.2830969.
- [4] S.-H. Hsu, Y.-J. Ren, and K. Chang, "A dual-polarized planar-array antenna for S-band and X-band airborne applications," *IEEE Antennas Propag. Mag.*, vol. 51, no. 4, pp.70-78, Aug. 2009, doi: 10.1109/MAP.2009.5338685.
- [5] M. Liu, Q. Wu, and Z.-R. Feng, "A millimeter-wave 4x4 conical conformal and dual-band microstrip array," in *Proc. Asia-Pacific Microw. Conf.*, Macau, Dec. 2008, pp. 1-4, doi: 10.1109/APMC.2008.4958558.

- [6] H. Schippers, J. Verpoorte, P. Jorna, A. Hulzinga, A. Meijerink, C. G. H. Roeloffzen, L. Zhuang, D. A. I. Marpaung, W. van Etten, R. G. Heideman, A. Leinse, A. Borreman, M. Hoekman, and M. Wintels, "Broadband conformal phased array with optical beam forming for airborne satellite communication," in *Proc. IEEE Aerospace Conf.*, Big Sky, MT, USA, Mar. 2008, pp. 1–17, doi: [10.1109/AERO.2008.4526305](https://doi.org/10.1109/AERO.2008.4526305).
- [7] T. Li, H. Yang, Y. Lei, S. Li, X. Cao, and D. Sun, "Broadband RCS reduction of microstrip antenna using conformal metasurface," in *Proc. Int. Appl. Comput. Electromagn. Soc. Symp. China (ACES)*, Nanjing, China, Aug. 2019, pp. 1–2, doi: [10.23919/ACES48530.2019.9060428](https://doi.org/10.23919/ACES48530.2019.9060428).
- [8] C. Chen and H. Zheng, "Design of a dual-band conformal antenna on a cone surface for missile-borne," in *Proc. 6th Asia-Pacific Conf. Antennas Propag. (APCAP)*, Xi'an, Oct. 2017, pp. 1–3, doi: [10.1109/APCAP.2017.8420994](https://doi.org/10.1109/APCAP.2017.8420994).
- [9] G. V. Ganesh, "Design of dual band comb shaped patch antenna with strip defected ground for wireless communications," in *Proc. 8th Int. Conf. Signal Process. Integr. Netw. (SPIN)*, Noida, India, Aug. 2021, pp. 992–997, doi: [10.1109/SPIN52536.2021.9566088](https://doi.org/10.1109/SPIN52536.2021.9566088).
- [10] G. Buttazzoni and R. Vesco, "Deterministic and stochastic approach to the synthesis of conformal arrays for SAR applications," in *Proc. Int. Conf. Electromagn. Adv. Appl. (ICEAA)*, Turin, Italy, Sep. 2013, pp. 520–523, doi: [10.1109/ICEAA.2013.6632292](https://doi.org/10.1109/ICEAA.2013.6632292).
- [11] F. Rostan and W. Wiesbeck, "Dual polarized microstrip patch arrays for the next generation of spaceborne synthetic aperture radars," in *Proc. Int. Geosci. Remote Sens. Symp. Quant. Remote Sens. Sci. Appl.*, Firenze, Italy, Jul. 1995, pp. 2277–2279, doi: [10.1109/IGARSS.1995.524170](https://doi.org/10.1109/IGARSS.1995.524170).
- [12] Y. Suo, Y. Liu, and W. Li, "Dual-band conformal antenna with omnidirectional radiation pattern on cylindrical surface," in *Proc. Int. Symp. Antennas Propag. (ISAP)*, Phuket, Oct. 2017, pp. 1–2, doi: [10.1109/ISANP.2017.8228797](https://doi.org/10.1109/ISANP.2017.8228797).
- [13] S. Weiyu, C. Guohu, and Z. Guangqiu, "Dual-band conformal meanderline monopole antenna with coupled patch for unmanned aerial vehicle applications," in *Proc. 11th Int. Symp. Antennas, Propag. EM Theory (ISAPE)*, Guilin, China, Oct. 2016, pp. 171–174, doi: [10.1109/ISAPE.2016.7833912](https://doi.org/10.1109/ISAPE.2016.7833912).
- [14] J. M. F. González, J. M. I. Alonso, J. G. Trujillo, A. N. S. de Toca, and M. S. Pérez, "GEODA-SARAS: Multi-phased array planar antenna design and measurements," in *Proc. 8th Eur. Conf. Antennas Propag. (EuCAP)*, The Hague, The Netherlands, Apr. 2014, pp. 423–425, doi: [10.1109/EuCAP.2014.6901782](https://doi.org/10.1109/EuCAP.2014.6901782).
- [15] P. Kabacik, G. Jaworski, M. Kamaszuk, P. Hornik, and T. Maleszka, "Lightweight conformal dual band antenna for spaceborne applications," in *Proc. 1st Eur. Conf. Antennas Propag.*, Nice, France, Nov. 2006, pp. 1–5, doi: [10.1109/EUCAP.2006.4585072](https://doi.org/10.1109/EUCAP.2006.4585072).
- [16] C.-X. Mao, S. Gao, and T. Rommel, "Low-profile aperture-shared X/Ka-band dual-polarized antenna for DBF-SAR applications," in *Proc. Int. Workshop Antenna Technol., Small Antennas, Innov. Struct., Appl. (iWAT)*, Athens, Greece, Mar. 2017, pp. 104–107, doi: [10.1109/IWAT.2017.7915329](https://doi.org/10.1109/IWAT.2017.7915329).
- [17] R. Pokuls, J. Uher, and D. M. Pozar, "Microstrip antennas for SAR applications," *IEEE Trans. Antennas Propag.*, vol. 46, no. 9, pp. 1289–1296, Sep. 1998, doi: [10.1109/8.719972](https://doi.org/10.1109/8.719972).
- [18] E. Lee, P. S. Hall, P. Gardner, and D. Kitchener, "Multi-band antennas," in *Proc. IEEE Antennas Propag. Soc. Int. Symp. Dig. Held Conjunct. USNC/URSI Nat. Radio Sci. Meeting*, Orlando, FL, USA, Jul. 1999, pp. 912–915, doi: [10.1109/APS.1999.789460](https://doi.org/10.1109/APS.1999.789460).
- [19] K. Kellogg, P. Hoffman, S. Standley, S. Shaffer, P. Rosen, W. Edelstein, C. Dunn, C. Baker, P. Barela, Y. Shen, A. M. Guerrero, P. Xaypraseuth, V. R. Sagi, C. V. Sreekantha, N. Harinath, R. Kumar, R. Bhan, and C. V. H. S. Sarma, "NASA-ISRO synthetic aperture radar (NISAR) mission," in *Proc. IEEE Aerosp. Conf.*, Big Sky, MT, USA, Mar. 2020, pp. 1–21, doi: [10.1109/AERO47225.2020.9172638](https://doi.org/10.1109/AERO47225.2020.9172638).
- [20] P. Hoffman, W. Edelstein, D. Arenas, S. Shaffer, R. Bhan, D. Kahn, J. Waldman, S. Nowak, V. Mora, P. Xaypraseuth, and B. Ferdowski, "NASA-ISRO synthetic aperture radar (NISAR) mission: System integration & test," in *Proc. IEEE Aerosp. Conf. (AERO)*, Big Sky, MT, USA, Mar. 2022, pp. 1–17, doi: [10.1109/AERO53065.2022.9843829](https://doi.org/10.1109/AERO53065.2022.9843829).
- [21] Y. F. Wu and Y. J. Cheng, "S-band dual circular polarized spherical conformal phased array antenna," in *Proc. IEEE Int. Workshop Electromagnetics: Appl. Student Innov. Competition (iWEM)*, Nanjing, China, May 2016, pp. 1–3, doi: [10.1109/iWEM.2016.7504911](https://doi.org/10.1109/iWEM.2016.7504911).
- [22] Z. Bao, Y.-X. Guo, and R. Mittra, "Single-layer dual-/tri-band inverted-F antennas for conformal capsule type of applications," *IEEE Trans. Antennas Propag.*, vol. 65, no. 12, pp. 7257–7265, Dec. 2017, doi: [10.1109/TAP.2017.2758161](https://doi.org/10.1109/TAP.2017.2758161).
- [23] C. Heer, C. Fischer, and C. Schaefer, "Spaceborne SAR systems and technologies," in *IEEE MTT-S Int. Microw. Symp. Dig.*, Anaheim, CA, USA, May 2010, pp. 538–541, doi: [10.1109/MWSYM.2010.5517840](https://doi.org/10.1109/MWSYM.2010.5517840).
- [24] G. Tyc, M. Grigorian, and R. Korus, "The SAR-XL multi-aperture X and L band SAR system with digital beamforming and its corresponding dual-band applications," in *Proc. IEEE Int. Geosci. Remote Sens. Symp.*, Waikoloa, HI, USA, Sep. 2020, pp. 3585–3588, doi: [10.1109/IGARSS39084.2020.9324300](https://doi.org/10.1109/IGARSS39084.2020.9324300).
- [25] J.-H. Bang, W.-J. Kim, and B.-C. Ahn, "Two-element conformal antenna for multi-GNSS reception," *IEEE Antennas Wireless Propag. Lett.*, vol. 16, pp. 796–799, 2017, doi: [10.1109/LAWP.2016.2604396](https://doi.org/10.1109/LAWP.2016.2604396).
- [26] C.-X. Mao, S. Gao, C. Tienda, T. Rommel, A. Patyuchenko, M. Younis, L. Boccia, E. Arneri, S. Glisic, U. Yodprasit, P. Penkala, M. Krstic, F. Qin, O. Schrape, A. Koczor, G. Amendola, and V. Petrovic, "X/Ka-band dual-polarized digital beamforming synthetic aperture radar," *IEEE Trans. Microw. Theory Techn.*, vol. 65, no. 11, pp. 4400–4407, Nov. 2017, doi: [10.1109/TMTT.2017.2690435](https://doi.org/10.1109/TMTT.2017.2690435).
- [27] A. M. Flashy, "Double-sided microstrip circular antenna array for radar applications," *Int. J. Eng. Res.*, vol. 2, no. 11, pp. 1805–1809, 2013.
- [28] F. Qin, S. S. Gao, Q. Luo, C.-X. Mao, C. Gu, G. Wei, J. Xu, J. Li, C. Wu, K. Zheng, and S. Zheng, "A simple low-cost shared-aperture dual-band dual-polarized high-gain antenna for synthetic aperture radars," *IEEE Trans. Antennas Propag.*, vol. 64, no. 7, pp. 2914–2922, Jul. 2016, doi: [10.1109/TAP.2016.2559526](https://doi.org/10.1109/TAP.2016.2559526).
- [29] C.-X. Mao, S. Gao, Y. Wang, Q. Luo, and Q.-X. Chu, "A shared-aperture dual-band dual-polarized filtering-antenna-array with improved frequency response," *IEEE Trans. Antennas Propag.*, vol. 65, no. 4, pp. 1836–1844, Apr. 2017, doi: [10.1109/TAP.2017.2670325](https://doi.org/10.1109/TAP.2017.2670325).
- [30] C.-X. Mao, S. Gao, Y. Wang, Q.-X. Chu, and X.-X. Yang, "Dual-band circularly polarized shared-aperture array for C-/X-band satellite communications," *IEEE Trans. Antennas Propag.*, vol. 65, no. 10, pp. 5171–5178, Oct. 2017, doi: [10.1109/TAP.2017.2740981](https://doi.org/10.1109/TAP.2017.2740981).
- [31] H. Y. Zeng, T. Xu, J. An, and B. F. Zong, "Calculation and simulation of antenna elements and 4-element sub-arrays operating in C/X band," *Proc. Comput. Sci.*, vol. 166, pp. 236–240, 2020, doi: [10.1016/j.procs.2020.02.107](https://doi.org/10.1016/j.procs.2020.02.107).
- [32] A. M. Yusuf, H. Wijanto, and Edwar, "Dual C-X-band E-shaped microstrip antenna array 1×8 for synthetic aperture radar on UAV," in *Proc. IEEE Int. Conf. Signals Syst. (ICSigSys)*, Bandung, Indonesia, Jul. 2019, pp. 186–189, doi: [10.1109/ICSIGSYS.2019.8811085](https://doi.org/10.1109/ICSIGSYS.2019.8811085).
- [33] B. A. Nunna and V. K. Kothapudi, "Design and analysis of X-band conformal antenna array for spaceborne synthetic aperture radar applications," in *Proc. 2nd Int. Conf. Comput. Electron. Wireless Commun.*, vol. 554, in Lecture Notes in Networks and Systems, S. Rawat, S. Kumar, P. Kumar, J. Anguera, Eds. Singapore: Springer Nature, 2023, pp. 193–204, doi: [10.1007/978-981-19-6661-3_18](https://doi.org/10.1007/978-981-19-6661-3_18).
- [34] B. A. Nunna and V. K. Kothapudi, "Design and analysis of 1 × 4 corporate feed conformal microstrip antenna array for X-band spaceborne synthetic aperture radar applications," in *Advances in Signal Processing, Embedded Systems and IoT* (Lecture Notes in Electrical Engineering), vol. 992, V. S. Chakravarthy, V. Bhateja, W. F. Fuentes, J. Anguera, K. P. Vasavi, Eds. Singapore: Springer Nature, 2023, pp. 93–102, doi: [10.1007/978-981-19-8865-3_8](https://doi.org/10.1007/978-981-19-8865-3_8).
- [35] B. A. Nunna and V. K. Kothapudi, "Design and analysis of single layer C/X-band conformal shared aperture antenna array for spaceborne SAR applications," in *Proc. IEEE Microw. Antennas Propag. Conf. (MAPCON)*, Bangalore, India, Dec. 2022, pp. 758–763, doi: [10.1109/MAPCON56011.2022.10047384](https://doi.org/10.1109/MAPCON56011.2022.10047384).
- [36] L. E. Vivanco-Benavides, C. L. Martínez-González, C. Mercado-Zúñiga, and C. Torres-Torres, "Machine learning and materials informatics approaches in the analysis of physical properties of carbon nanotubes: A review," *Comput. Mater. Sci.*, vol. 201, Jan. 2022, Art. no. 110939, doi: [10.1016/j.commatsci.2021.110939](https://doi.org/10.1016/j.commatsci.2021.110939).
- [37] M. M. Khan, S. Hossain, P. Mozumdar, S. Akter, and R. H. Ashique, "A review on machine learning and deep learning for various antenna design applications," *Heliyon*, vol. 8, no. 4, Apr. 2022, Art. no. e09317, doi: [10.1016/j.heliyon.2022.e09317](https://doi.org/10.1016/j.heliyon.2022.e09317).

- [38] D. Park and J. Choi, "A dual-band dual-polarized antenna with improved isolation characteristics for polarimetric SAR applications," *Appl. Sci.*, vol. 11, no. 21, p. 10025, Oct. 2021, doi: [10.3390/app112110025](https://doi.org/10.3390/app112110025).
- [39] M. Dwivedi and D. K. Vishwakarma, "A conformal phased array antenna with improved gain on a cylindrical surface," *IETE J. Res.*, pp. 1–9, Jul. 2023, doi: [10.1080/03772063.2023.2232790](https://doi.org/10.1080/03772063.2023.2232790).



VENKATA KISHORE KOTHAPUDI (Senior Member, IEEE) was born in Tenali, Guntur, Andhra Pradesh, India, in 1987. He received the Graduate degree in electronics and communication engineering from TPIST, JNTU Hyderabad, India, in 2008, the M.Tech. degree in communication and radar systems from KLEF, India, in 2012, and the Ph.D. degree from the Microwave Division, School of Electronics Engineering (SENSE), Vellore Institute of Technology (VIT), Vellore,

Tamil Nadu, India. He is currently an Associate Professor with the Department of Electronics and Communication Engineering, Vignan's Foundation for Science, Technology and Research (VFSTR), Vadlamudi, Guntur. He has published more than 15 research papers in international journals and national and IEEE international conferences. He has been the author and the coauthor of many IEEE proceeding papers. He has published research papers in IEEE ACCESS, with a 3.557 impact factor; *IET Microwave, Antennas and Propagation*, the *Progress in Electromagnetic Research (PIER)* international journal, *Journal of Electromagnetic Engineering and Science (JEES)*, and IEEE international conferences. He is a Reviewer for several reputed journals, such as IEEE ACCESS, IET journals, *Electronic Letters*, *IJCS* (Wiley), Springer journals, *JEES*, *ACES*, *Advanced Electromagnetics*, and *JESTR*. He traveled to Sri Lanka and Singapore for the IEEE SYWC 2015 meeting and the IEEE APSAR 2015 Conference, respectively, to present his research work and as a part of his research. He has more than seven years of research and industry experience in RF and microwave engineering in ECIL as a GEA and NARLISRO and a Project Student and an Engineer with Astra Microwave Products. He has a rich experience on radar systems design, which includes transmit/receive modules [HF, VHF, L, S, and C-Band], RF and microwave feeder network and beam forming, RF and microwave active and passive components, RF power amplifiers, antenna system, which includes Yagi-Uda and microstrip patch antenna as a phased array with different configurations by using analysis and synthesis techniques. His research interests include shared aperture antenna technology (single layer and multilayer-L/S/C/X/K-bands) for radar engineering includes airborne and space borne synthetic aperture radar and radar wind profilers. He is a Senior Member of the American Institute of Aeronautics and Astronautics (AIAA) and Applied Computational Electromagnetics Society (ACES). He is associated with IEEE societies (AP-s., MTT-s., AES-s., GRS-s., IP-s., and ComSoc & EMC-s).

...



BALA ANKAIYAH NUNNA (Graduate Student Member, IEEE) was born in Mundlapadu, Prakasam, Andhra Pradesh, India, in 1992. He received the Graduate degree in electronics and communication engineering from ANU, Guntur, India, in 2012, and the M.Tech. degree in digital electronics and communication systems from JNTU Kakinada, India, in 2019. He is currently a Research Scholar with the Department of Electronics and Communication Engineering,

Vignan's Foundation for Science, Technology and Research (VFSTR), Vadlamudi, Guntur, Andhra Pradesh. He has published 14 research papers in international journals and national and IEEE international conferences. He has been the author and the coauthor of many IEEE proceeding papers. His research interests include conformal shared aperture antenna technology (single layer and multilayer-L/S/C/X/K-bands) for radar engineering includes airborne and space borne synthetic aperture radar. He is associated with IEEE societies (AP-s. and MTT-s).